Time-of-flight neutron-scattering study of $YbInCu_4$ and $YbIn_{0.3}Ag_{0.7}Cu_4$

J. M. Lawrence
University of California, Irvine, California 92697

R. Osborn
Argonne National Laboratory, Argonne, Illinois 60439

J. L. Sarrao
Los Alamos National Laboratory, Los Alamos, New Mexico 87545

Z. Fisk
Florida State University, Tallahassee, Florida 32306
(Received 24 August 1998)

We report neutron-scattering experiments for $YbInCu_4$ that were performed in the time-of-flight mode at a neutron spallation source. Two independent methods were used to determine the nonmagnetic scattering and both gave comparable results for the magnetic scattering. The magnetic scattering was measured at temperatures $T=30$ and 60 K, below and above the temperature of the valence transition $T_s=40$ K. Our key result is that the spin dynamics in the mixed valent phase are well described over a broad range of energy transfer ($10<\Delta E<150$ meV) and incident energies ($35 \leqslant E_i \leqslant 150$ meV) by a Lorentzian power spectrum, centered at $E_0 \cong 40$ meV, and with halfwidth $\Gamma \cong 13$ meV. The magnetic susceptibility derived from the fits is within 20% of the value measured for the dc susceptibility. The peak energy is in good agreement with the Kondo temperature derived from thermodynamic studies but the Lorentzian line shape fits the data significantly better ($\chi^2 \cong 2$) than the line shape expected for a Kondo impurity ($\chi^2 \cong 10$). In addition we report results for $YbIn_{0.3}Ag_{0.7}Cu_4$. For this compound, the scattering is inelastic at low temperature (at 10 K $E_0=7.4$ meV, and $\Gamma=7.6$ meV) but is quasielastic at higher temperature where $\Gamma=10.0$ and 13.2 meV at 150 and 300 K, respectively. This increase in linewidth is contrary to the 50% decrease in linewidth predicted by the Anderson impurity model for this temperature range, and is also smaller than the factor of four increase in characteristic energy suggested by application of the impurity model to the magnetic susceptibility.
[S0163-1829(99)04002-3]

INTRODUCTION

The compound $YbInCu_4$ has a first order valence transition at $T_s=40$ K where the Yb changes from a nearly trivalent ($z=2.96$) local moment paramagnetic state with small Kondo temperature ($T_K \sim 25$ K) at high temperature to a mixed-valent ($z=2.82$) Pauli paramagnetic state with large Kondo temperature ($T_K \sim 400$ K) at low temperature[1–3] [Fig. 1(a)]. Following an older study[4] of the spin dynamics performed on a polycrystalline sample, we recently studied[5] a single crystal on a triple axis spectrometer for energy transfers up to 65 meV. For $T>T_s$ the scattering shows a peak at $E_0^+=2.3$ meV with a halfwidth of $\Gamma_+=1.8$ meV; this can be attributed to a crystal field excitation that is broadened by $4f$/conduction electron hybridization. For $T<T_s$, the power function appears to be Lorentzian, centered at $E_0^-=40.2$ meV and with a halfwidth of $\Gamma_-=12.3$ meV. The peak energies are consistent with the Kondo energies deduced from the susceptibility. The line shape and intensity of the scattering is independent of momentum transfer Q for both phases.

The purpose of the current study is to study the scattering over a wider range of energy transfer and with improved statistics in order to more accurately determine the power function. This is an issue of general interest in the study of mixed-valent compounds. Theoretical predictions for an Anderson impurity suggests that the power function is nearly Lorentzian for values of the $4f$ occupation number n_f close to unity. (For Yb, n_f is the number of holes in the $4f$ shell; i.e., $n_f=1$ for the trivalent $4f^{13}$ configuration and $n_f=0$ for the divalent nf^{14} configuration.) According to theory the ratio Γ/E_0 of the linewidth to the excitation energy is set by n_f, hence in order to test the validity of these predictions the line shape needs to be determined in conjunction with experimental determination of n_f. Furthermore, in order to put strong constraints on the line shape it is necessary to determine the magnetic scattering over a wide dynamic range of energies; measurements over a range of energy transfer small compared to the characteristic energy scale for the spin fluctuations will not provide a stringent test of theory. In this regard we note that the earlier studies of the scattering extended to energy transfers ($\Delta E_{max}=50$ and 65 meV for Refs. 4 and 5, respectively) only slightly larger than $E_0^-=40$ meV.

The compound $YbInCu_4$ has several advantages for such a study. The major uncertainty in determining the magnetic scattering in powder samples comes from the correction for the nonmagnetic scattering. The earlier studies show that the scattering peak in mixed-valent $YbInCu_4$ occurs at energies larger than the phonon cutoff beyond which energy the non-
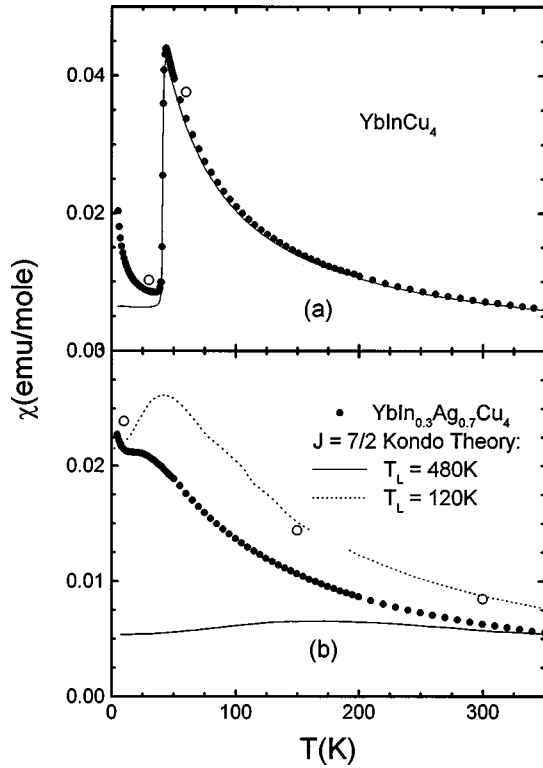
FIG. 1. (a) The dc magnetic susceptibility $\chi(T)$ of the YbInCu$_4$ sample used in the current study (solid circles). The solid line represents $\chi(T)$ after correction for an impurity Curie term. The open circles are the values for the susceptibility derived from the fits to the spin dynamics in Figs. 6(a) and 6(d). (b) The dc susceptibility of YbIn$_{0.3}$Ag$_{0.7}$Cu$_4$ (solid circles). The open circles are derived from the fits to the spin dynamics in Fig. 8. The solid and dashed lines are $J = \frac{7}{2}$ Kondo curves (Ref. 17) for two Kondo temperatures $T_L = C_{7/2}/\chi(0)$ where $C_{7/2}$ is the Yb $J = \frac{7}{2}$ Curie constant.

magnetic background, including multiple scattering, is fairly small. In addition, the change in the lattice parameter at the phase transition is very small ($\Delta V/V = 0.005$) so that changes in the nonmagnetic scattering are also small; this allows for an independent subtraction procedure for removal of the nonmagnetic scattering (see below). In the present study we use time-of-flight neutron scattering at a spallation source to study the spin dynamics. This has allowed us to extend the region of energy transfer to 150 meV, significantly larger than the peak energy (40 meV). Taking advantage of the fact that the spin dynamics have been shown to be Q independent we have averaged the data over scattering angle in order to improve the counting statistics. The major disadvantage presented by YbInCu$_4$ for this measurement is that the neutron absorption is large, due to the presence of In.

In the system YbIn$_{1-x}$Ag$_x$Cu$_4$ for $x < 0.5$ the $4f$-$4f$ interactions responsible for the valence transition cause a rapid change of the valence with temperature but for $x > 0.5$ the change of valence with temperature is weak and in accord with the predictions of the single-impurity Anderson model.[3] Single impurity theory does not, however, provide a good fit to the susceptibility for YbIn$_{0.3}$Ag$_{0.7}$Cu$_4$: the fits suggest a larger T_K at room temperature than at low temperature [Fig. 1(b)]. We have included a study of YbIn$_{0.3}$Ag$_{0.7}$Cu$_4$ to test whether this failure of the single-ion theory can be explained by an actual change in the characteristic energy.

EXPERIMENTAL DETAILS

The neutron-scattering measurements were performed in the time-of-flight mode at the Low Resolution Medium Energy Chopper Spectrometer (LRMECS) (Ref. 6) at the Intense Pulsed Neutron Source (IPNS) at Argonne National Laboratory. Single crystals of YbInCu$_4$ (LuInCu$_4$) and YbIn$_{0.3}$Ag$_{0.7}$Cu$_4$ (LuIn$_{0.3}$Ag$_{0.7}$Cu$_4$) were grown in InCu and In$_{0.3}$Ag$_{0.7}$Cu fluxes, as reported earlier.[2] A large number of crystals of total mass ≈ 50 g were crushed into a powder and loaded into rectangular (7.5×10 cm) thin-walled aluminum containers. The susceptibility (Fig. 1) of a representative sample of this powder was measured in a SQUID magnetometer as a check of sample quality. The mean thickness of the samples was $1–2$ mm with some nonuniformity due to granularity. The holder was mounted on the cold finger of a closed cycle (Displex) refrigerator for temperature control. Spectra were obtained for a number of incident energies ($E_i = 15, 35, 60,$ and 150 meV and $T = 30$ and 60 K for YbInCu$_4$, $E_i = 25$ and 80 meV and $T = 10, 150,$ and 300 K for YbIn$_{0.3}$Ag$_{0.7}$Cu$_4$). Typical scans lasted 24 h. At each incident energy we also measured the spectra of LuInCu$_4$ or LuIn$_{0.3}$Ag$_{0.7}$Cu$_4$ to help determine the nonmagnetic scattering, the empty sample holder to determine the background scattering and a vanadium foil. The latter was used to calibrate the scattering function $S(\phi, \Delta E)$ (in mb/sr meV) with an absolute accuracy of $10–20$ %. The resolution width (FWHM) is in the range $0.05–0.1 E_i$ for elastic scattering, depending on incident energy and scattering angle; this width decreases smoothly as a function of energy transfer ΔE, and is a factor of $4–5$ smaller when $\Delta E = E_i$. For the results reported below we have taken advantage of the earlier observation[5] that the magnetic scattering is independent of the momentum transfer Q and we have summed the counts in three groups of detectors at average scattering angles $\phi = 20°, 60°,$ and $100°$. The momentum transfer increases uniformly with scattering angle ϕ and is also a function of energy transfer: for the relevant range of energy transfer, Q is in the range $1–2$ Å^{-1} for $\phi = 20°$ and $4–7$ Å^{-1} for $\phi = 100°$ when $E_i = 15–35$ meV; $2–3$ Å^{-1} for $\phi = 20°$ and $7–10$ Å^{-1} for $\phi = 100°$ when $E_i = 60–80$ meV; and $3–4$ Å^{-1} for $\phi = 20°$ and $10–15$ Å^{-1} for $\phi = 100°$ when $E_i = 150$ meV. Since the Yb $4f$ form factor decreases the magnetic scattering intensity while the phonon scattering grows rapidly as Q increases, the magnetic scattering should dominate at $\phi = 20°$ and the phonon scattering should dominate at $\phi = 100°$. Due to the presence of In in the samples, there is considerable neutron absorption. For the plots shown below (with the exception of Fig. 6) we have not corrected the data for this absorption; since fewer neutrons are incident on the holder due to the sample absorption, we have performed an inverse correction for the empty sample holder. The data in Fig. 6 and the fits in Figs. 5 and 8 have been corrected for absorption assuming a rectangular sample of uniform thickness.

RESULTS AND ANALYSIS: YbInCu$_4$

In Fig. 2 the scattering is shown for two incident energies for temperatures above and below $T_s = 40$ K, and at low scattering angle where the magnetic scattering dominates. The
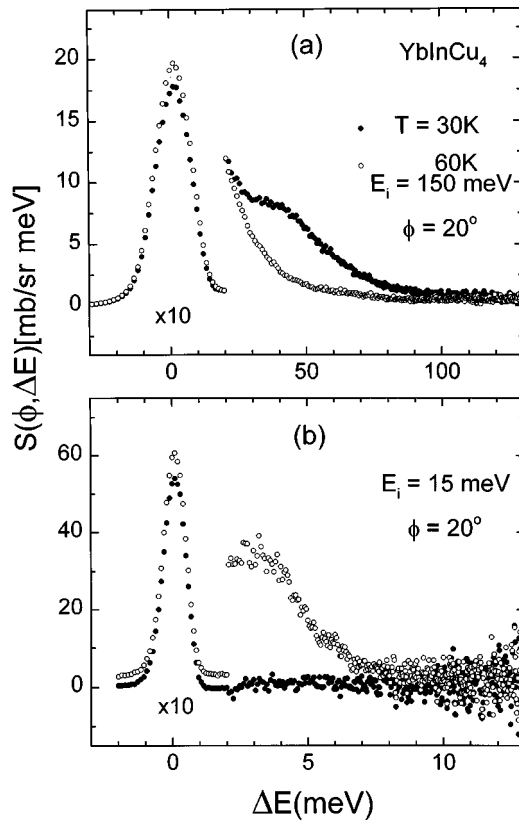
FIG. 2. The experimental scattering function $S(\phi, \Delta E)$ for YbInCu$_4$ at low scattering angle $\phi = 20°$ for two temperatures above and below the temperature $T_s = 40$ K of the valence transition and for two incident energies $E_i = 150$ and 15 meV. The scattering from the empty holder has been subtracted from the data.

low temperature scattering exhibits a broad peak centered near 40 meV. For $T > T_s$ this peak disappears and is replaced by a peak near 3 meV; this increase in the magnetic scattering at low energy transfer also causes the elastic peak height to increase. This change in the characteristic energy of the magnetic scattering from a large value at low temperature to a small value at high temperature is a basic feature of the valence transition.[2–5]

In Fig. 3 we exhibit the scattering for $E_i = 60$ meV and $T = 30$ K as a function of scattering angle. For $\phi = 100°$ the scattering is dominated by phonon scattering, peaking near 15 meV. For $\phi = 20°$ the phonon peak is strongly reduced and the magnetic peak at 40 meV dominates. At intermediate scattering angle, there is an equal admixture of these two types of scattering. The nonmagnetic contribution (phonon scattering, including multiple scattering) can be seen in the results for the nonmagnetic analog compound LuInCu$_4$ (Fig. 4). The scattering for LuInCu$_4$ is quite similar to that of YbInCu$_4$; e.g., at $E_i = 60$ meV and $\phi = 100°$ both show a main peak near 15 meV (which coincides with the optic phonon branch in the [1,0,0] direction observed in the earlier study of a single crystal) and a secondary peak near 8 meV and the scattering vanishes above 35 meV. The integrated intensity for the LuInCu$_4$ scattering scales with scattering angle approximately linearly with Q; the Q^2 dependence expected on the basis of the incoherent approximation is modified by multiple scattering and absorption.

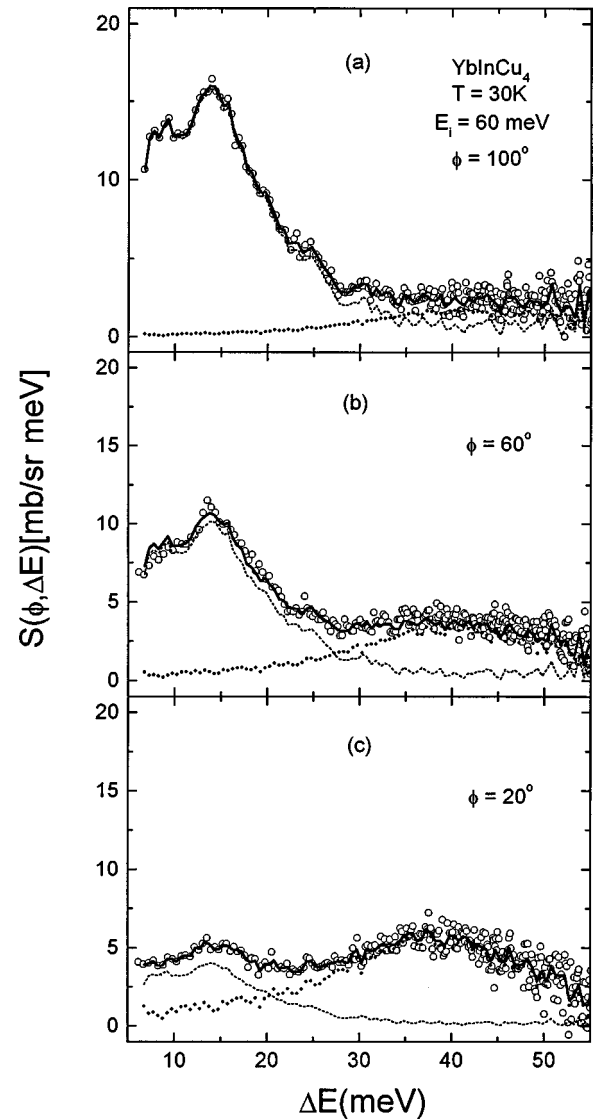For each incident energy we have determined the non-

FIG. 3. The low temperature ($T = 30$ K) scattering function for YbInCu$_4$ at $E_i = 60$ meV and for three scattering angles (open circles). The dotted lines (dashed lines) represent the magnetic (nonmagnetic) scattering derived as described in the text; the solid line is the sum of the magnetic and nonmagnetic scattering.

magnetic and magnetic scattering for YbInCu$_4$ under the assumptions that the magnetic scattering scales with scattering angle and energy transfer in the same manner as the Yb $4f$ form factor and the integrated phonon scattering scales with scattering angle in the same way as in LuInCu$_4$. This latter assumption has been shown to give a good account of the combined effect of the phonon Q dependence and the multiple scattering.[7] A typical example is shown in Fig. 3; the magnetic scattering (dotted line) and phonon scattering (dashed line) are determined self-consistently from the data at $\phi = 20°$ and 100° and the total fit at $\phi = 60°$ serves as a consistency check on the procedure. The magnetic scattering obtained in this manner for $E_i = 35$, 60, and 150 meV is plotted in Fig. 5. Although the width of the elastic peak is $\sim 0.07 E_i$ (FWHM) the wings of the elastic peak are appreciable for $E < 0.2 E_i$; these wings are poorly determined in energy loss and, since the elastic incoherent scattering is strong in these compounds, they lead to uncertainty in the
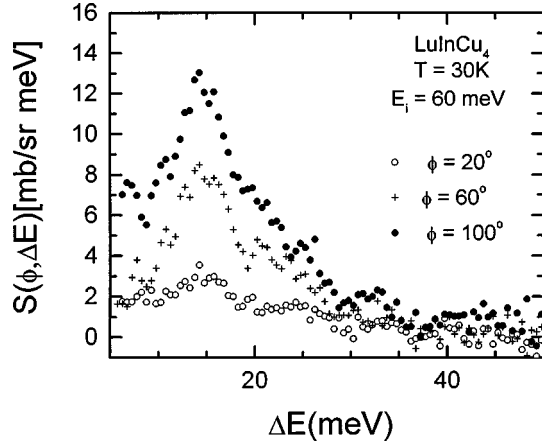
FIG. 4. The low temperature ($T = 30$ K) scattering function for LuInCu$_4$ at $E_i = 60$ meV and at three scattering angles.

magnetic scattering for this range of energy transfer. Hence we have restricted the data in Fig. 5 to energies greater than $0.2E_i$.

The magnetic scattering obeys the following relation:

$$S_{mag}(Q, \Delta E, T) = A\chi(Q;T)[n(\Delta E;T)$$
$$+ 1]f^2(Q)\Delta E P(\Delta E;T). \qquad (1)$$

Here, $A = (2N/\mu_B^2), \chi(Q;T)$ is the static susceptibility, $[n(\Delta E;T) + 1]$ is the Bose factor, $f^2(Q)$ is the Yb $4f$ form factor and $P(\Delta E)$ is the normalized power function. We noted above that changes in the lattice are very small at the phase transition. Under the assumption that the nonmagnetic scattering does not change at the phase transition, we can subtract the experimental scattering function $S(Q, \Delta E, T)$ for temperatures $T_+ > T_s$ and $T_- < T_s$ as a second method[8] for eliminating the nonmagnetic scattering:

$$\Delta S_{mag}(Q, \Delta E) \equiv S_{mag}(Q, \Delta E, T_-) - S_{mag}(Q, \Delta E, T_+)$$
$$\approx S(Q, \Delta E, T_-) - S(Q, \Delta E, T_+). \qquad (2)$$

Data for ΔS_{mag} are plotted for four incident energies in Fig. 6. We have excluded data for $-0.1E_i < \Delta E < 0.1E_i$, where the strong elastic scattering leads to errors in ΔS_{mag}.

In the fits shown in Figs. 5 and 6 we assume[5,6] that the normalized power spectrum is Lorentzian:

$$P(\Delta E;T) = (\Gamma/2\pi)\{[(\Delta E - E_0)^2 + \Gamma^2]^{-1}$$
$$+ [(\Delta E + E_0)^2 + \Gamma^2]^{-1}\} \qquad (3)$$

and we assume that the static susceptibility is Q independent. The fits account for the variation of Q with ΔE in the time of flight scan at the given scattering angle; they account for neutron absorption; and the fit functions are convolved with the instrumental resolution function. In fitting to ΔS_{mag} we assume that the power function obeys Eq. (3) at both $T_- = 30$ K and $T_+ = 60$ K. For the given resolution, inclusion of an additional quasielastic component at 60 K, as suggested by the earlier study,[4] did not significantly improve the fits; since our focus is on the ground state ($T < T_s$) we assume Eq. (3) for $T > T_s$ for simplicity. The values for the parameters at $T_+ = 60$ K are primarily derived from the fit [Fig. 6(d)] at $E_i = 15$ meV; they are $E_0^+ = 2.6$ meV, Γ_+
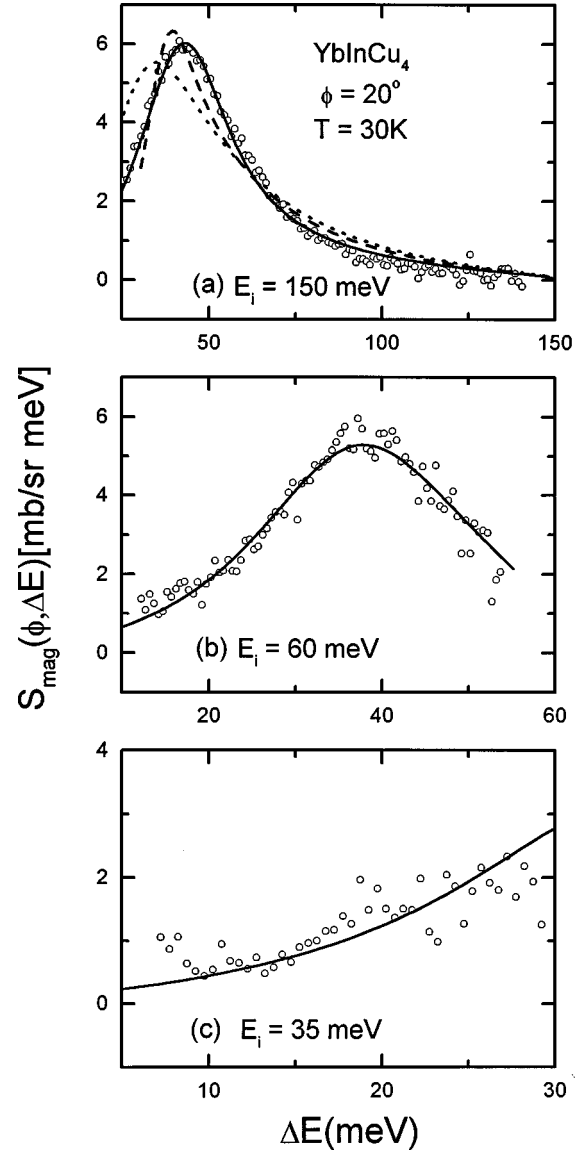

FIG. 5. The low temperature ($T = 30$ K) magnetic scattering for YbInCu$_4$, derived as in Fig. 3, for three incident energies $E_i = 35$, 60, and 150 meV and at low scattering angle $\phi = 20°$ (open circles). The solid lines are the results of fits to Eq. (1) assuming a Lorentzian power spectrum [Eq. (3)]. In the fits for $E_i = 60$ meV (35 and 150 meV), the parameters E_0 and Γ are constrained to the values $E_0 = 36.2(39.9)$ meV and $\Gamma = 16.4(13.5)$ meV, derived from the fits to ΔS_{mag} in Fig. 6(b) (a). The values of the parameter $\chi(30$ K$)$ derived from the fit are 9.9, 10.2, and 10.0×10^{-3} emu/mol for $E_i = 35$, 60, and 150 meV, respectively. The dotted line in (a) is a best fit of the KMH (Ref. 12) theoretical line shape for $n_f = 0.8$ where n_f is the Yb $4f$ hole occupation number; the dashed line is the best KMH fit for unconstrained n_f, with the result $n_f = 0.03$.

$= 1.6$ meV, and $\chi(60$ K$) = 37.6 \times 10^{-6}$ emu/mol. The fits at $E_i = 60$ and 150 meV [Figs. 6(a) and 6(b)] were performed by constraining the parameters for $T_+ = 60$ K to the values stated above. The resulting values for $T_- = 30$ K obtained for $E_i = 150$ meV were $E_0^- = 39.9$ meV, $\Gamma_- = 13.5$ meV and $\chi(30$ K$) = 10.4 \times 10^{-3}$ emu/mol. These values for $\chi(30)$ and $\chi(60)$ are plotted in Fig. 1(a). For $E_i = 60$ meV the values were $E_0^- = 36.2$ meV, $\Gamma_- = 16.4$ meV and $\chi(30$ K$) = 11.5 \times 10^{-3}$ emu/mol. In the plot [Fig. 6(c)] for $\Delta E = 35$ meV we
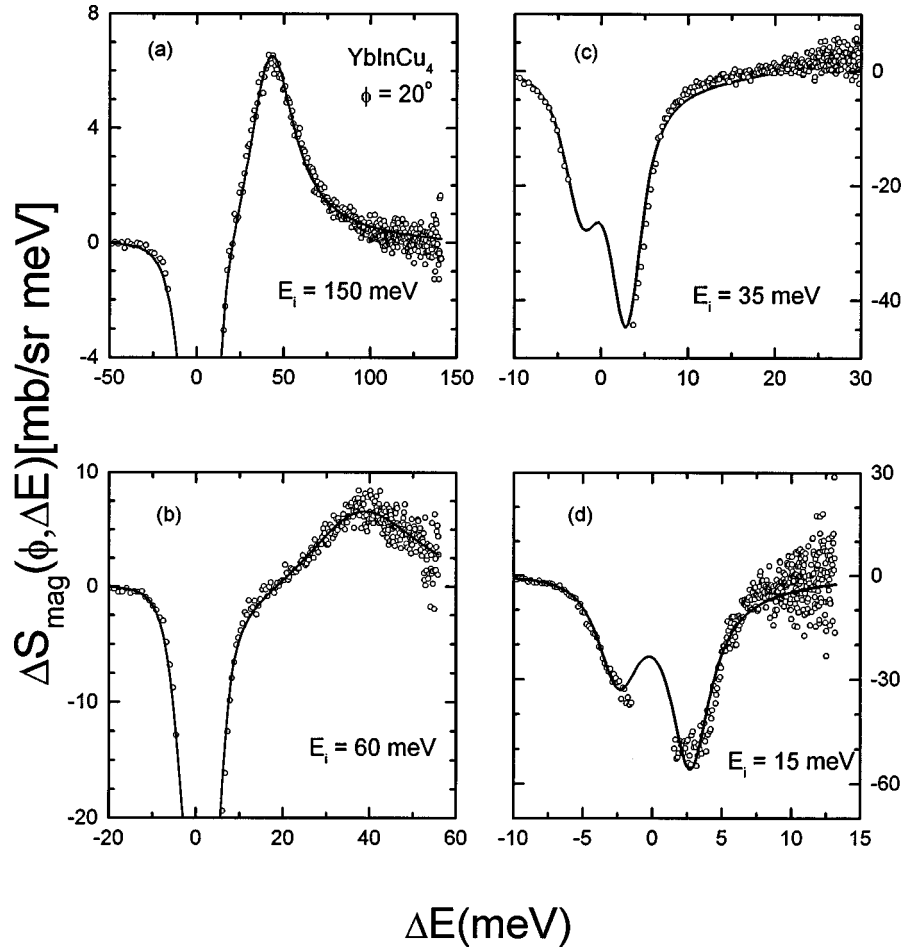
FIG. 6. The difference $\Delta S_{\text{mag}} = S(30\,\text{K}) - S(60\,\text{K})$ between the low angle ($\phi = 20°$) scattering above and below the valence transition for four incident energies (open circles); the data have been corrected for absorption. The solid lines represent fits to Eqs. (1) and (2) assuming Lorentzian power spectra [Eq. (3)] at both $T = 30$ and 60 K. The values for the parameters at 60 K are $E_0^+ = 2.6$ meV, $\Gamma_+ = 1.6$ meV, and $\chi(60\,\text{K}) = 37.6 \times 10^{-3}$ emu/mol. In (a), (c), and (d) the parameters for $T = 30$ K are $E_0^- = 39.9$ meV, $\Gamma_- = 13.5$ meV, and $\chi(30\,\text{K}) = 10.4 \times 10^{-3}$ emu/mol. For (b) the parameters at 30 K are $E_0^- = 36.2$ meV, $\Gamma_- = 16.4$ meV, and $\chi(30\,\text{K}) = 11.5 \times 10^{-3}$ emu/mol.

have constrained all parameters to those of Fig. 6(d). In the fits for Fig. 5 we have constrained the parameters E_0 and Γ to the values obtained from the fits to ΔS_{mag} at the given incident energy and varied only χ. The resulting values for susceptibility are $\chi(30\,\text{K}) = 9.9$, 10.2, and 10.0 $\times 10^{-3}$ emu/mol for $E_i = 35$, 60, and 150 meV, respectively. For all fits the values of reduced χ^2 were in the range 1.5–2.

For YbIn$_{0.3}$Ag$_{0.7}$Cu$_4$ we again equated the factor by which the nonmagnetic scattering scales with scattering angle to that measured in LuIn$_{0.3}$Ag$_{0.7}$Cu$_4$ at each incident energy (25 and 80 meV) and we determined the nonmagnetic and magnetic scattering self-consistently from the data for $\phi = 20°$ and 100°. Results for $E_i = 25$ meV and $T = 10$ K are shown for three scattering angles in Fig. 7. The sum of these two contributions at $\phi = 60°$ is 10% lower than the data for $10 < \Delta E < 20$ meV. It is harder here than for YbInCu$_4$ to determine the nonmagnetic scattering, both because it strongly overlaps the magnetic scattering, and because at this low incident energy the momentum transfer at $\phi = 100°$ is relatively small ($Q \sim 4-5$ Å^{-1}) so that the nonmagnetic and magnetic scattering are equally weighted at high scattering angle. To obtain the nonmagnetic scattering at higher temperatures, we simulated the nonmagnetic scattering (phonons plus multiple scattering) obtained at 10 K using Monte Carlo

calculations[7] and then used further calculations to scale the nonmagnetic scattering to higher temperature. The resulting magnetic scattering is shown for three temperatures in Fig. 8. In fitting the data of Fig. 8, we included all data shown for both incident energies. We again excluded the region $-0.2E_i < \Delta E < 0.2E_i$ from the fit because of the uncertainty in the elastic scattering. The Lorentzian power spectrum gives a reasonable representation of the data for $T = 10$ K, with $E_0 = 7.4$ meV and $\Gamma = 7.6$ meV; for $T = 150$ and 300 K, the quasielastic Lorentzian [i.e., $E_0 = 0$ in Eq. (3)] gives the best fit, with $\Gamma = 10.0$ meV at 150 K and 13.2 meV at 300 K. The values of susceptibility ($\chi = 23.9$, 14.4, and 8.4 $\times 10^{-3}$ emu/mol at 10, 150, and 300 K, respectively) obtained from the fit are plotted in Fig. 1.

DISCUSSION

In the oldest studies[9,10] of the spin dynamics of mixed valent compounds, the power function was assumed to be quasielastic [$\chi''(E) \propto E/(E^2 + \Gamma^2)$]. Subsequent theoretical work[11,12] showed that the power function should be inelastic at low temperatures and quasielastic only for $T > T_K$. The experimental magnetic scattering seen in α-Ce (Ref. 8) and α-Ce$_{1-x}$Th$_x$ (Ref. 6) can be fit with an inelastic Lorentzian
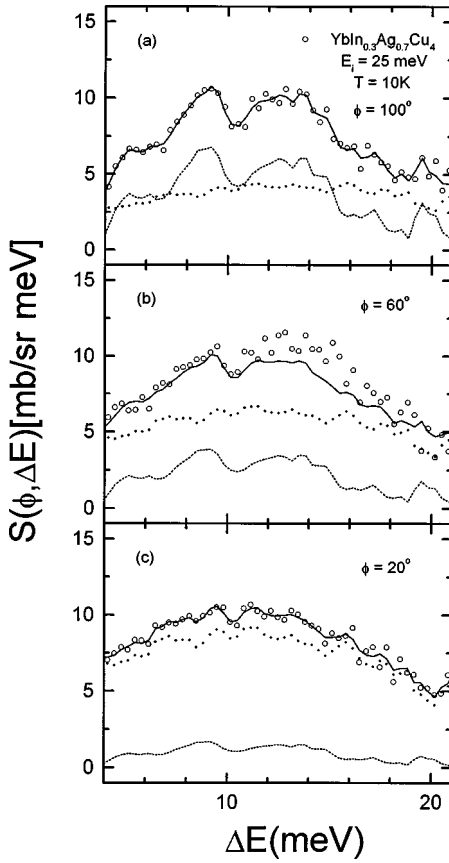
FIG. 7. The experimental scattering in $YbIn_{0.3}Ag_{0.7}Cu_4$ at $T = 10$ K and $E_i = 25$ meV for three scattering angles (open circles). As in Fig. 3 the dotted (dashed) lines represent magnetic (nonmagnetic) scattering, and the solid lines represent the sum of magnetic and nonmagnetic scattering.

FIG. 8. The low angle ($\phi = 20°$) magnetic scattering in $YbIn_{0.3}Ag_{0.7}Cu_4$ for three temperatures. The open circles were derived from data taken at incident energy $E_i = 80$ meV; the closed circles were obtained from the data taken at $E_i = 25$ meV. The solid lines are the fits to Eqs. (1) and (3) (Lorentzian power spectrum). The values of the parameters obtained from these fits are $E_0(10$ K$) = 7.4$ meV, $\Gamma(10$ K$) = 7.6$ meV, and $\chi(10$ K$) = 23.9 \times 10^{-3}$ emu/mol; $E_0(150$ K$) = 0$, $\Gamma(150$ K$) = 10.0$ meV and $\chi(150$ K$) = 14.4 \times 10^{-3}$ emu/mol; $E_0(300$ K$) = 0$, $\Gamma(300$ K$) = 13.2$ meV and $\chi(300$ K$) = 8.4 \times 10^{-3}$ emu/mol.

power spectrum [as in Eq. (3)]. On the other hand, the line shape for $CePd_3$ is a matter of controversy[13,14] and for $CeSn_3$ (Ref. 15) and $YbAl_3$ (Ref. 16) the line shape appears to have a second component in addition to the inelastic Lorentzian. Hence characterization of the line shape in $YbInCu_4$ is of general interest for the study of mixed valence.

In the fits (Figs. 5 and 6) to the magnetic scattering in $YbInCu_4$ using a Lorentzian power spectrum there are minor differences between the parameters Γ, E_0, and $\chi(T)$ obtained at $E_i = 60$ and 150 meV and between the values of $\chi(30$ K$)$ obtained by the two methods of subtracting the nonmagnetic scattering; furthermore the values obtained for χ at 30 and 60 K are larger than the dc susceptibility [Fig. 1(a)]. These differences reflect uncertainties in the subtraction of the nonmagnetic scattering, in the absorption correction (due to the nonuniformity of the sample thickness) and in the vanadium calibration. They may also reflect as-yet undetermined Q dependence of the scattering on the 15% level.[5] Determination of the magnetic scattering could be improved by studies at a higher intensity source, with concomitant better resolution and statistics. Determination of the low energy line shape at 60 K clearly requires higher resolution ($\Delta E \sim 0.1$ meV); the results of Ref. 4 are clearly superior to ours in this respect. Since these compounds are strongly absorbing, use of a uniformly thick sample would improve the absorption correction and the absolute calibration. However, the most significant problem in determining the magnetic
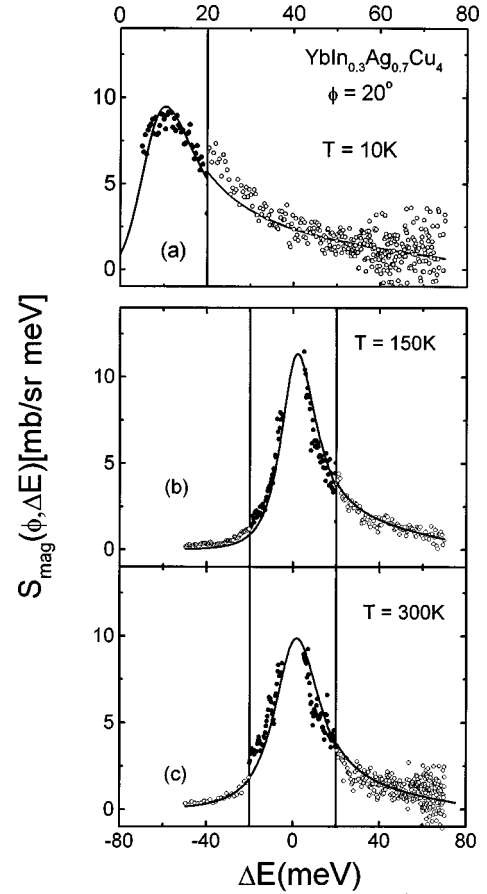
scattering in mixed valent compounds is correct determination of the nonmagnetic scattering. This requires knowledge of the phonon dispersion and calculation of the effects of multiple scattering and absorption, ideally without recourse to the incoherent approximation.

Nevertheless it is clear that the Lorentzian power spectrum, with $E_0 \approx 40$ meV and $\Gamma \approx 13$ meV gives consistent fits to the data over a wide range of energy transfer, for a wide range of incident energies, and for the two independent methods of subtracting the nonmagnetic scattering. The parameters are also in good agreement with those obtained from the earlier studies on polycrystal[4] and single crystal[5] samples. Hence, we believe our results provide a better-than-average case for comparison to theory.

The theoretical line shape for the single impurity Anderson model derived by Kuramoto and Müller-Hartmann[12] (KMH) is nearly Lorentzian, but the details of the line shape depend on the degeneracy $2J + 1$ and on the $4f$ occupation number n_f. We have determined[3] the latter experimentally to be $n_f = 0.8$ for $YbInCu_4$. For this value of n_f and for $2J + 1 = 8$, the peak in the KMH power spectrum should occur

at $1.1kT_L$ and the width should be $0.6kT_L$ where kT_L is a characteristic (Kondo) energy related to the ground state susceptibility by $\chi(0)=n_f C_{7/2}/T_L$. (Here $C_{7/2}$ is the $J=\frac{7}{2}$ Curie constant for Yb, 2.58 emu K/mol.) For the peak position $E_0=40$ meV, this leads to predicted values for $T_L=420$ K and for the susceptibility $\chi(0)=5\times10^{-3}$ emu/mol, which is in reasonable agreement with the value 6×10^{-3} emu/mol seen in the cleanest YbInCu$_4$ samples[2] [and seen in the present sample after subtraction of a Curie tail as in Fig. 1(a)].

On the other hand the present fits confirm a point made in the earlier single-crystal study: the ratio $\Gamma/E_0=0.32$ observed for our data is significantly smaller than the value 0.52 predicted by the KMH theory for $n_f=0.8$ and $J=\frac{7}{2}$. Indeed, the simple Lorentzian [solid line Fig. 5(a)] provides a significantly better fit to the data, with $\chi^2=2.1$, than the best fit of the KMH power function for $n_f=0.8$ [dotted line in Fig. 5(a)] where $\chi^2=11.1$. Indeed, the best fit of the KMH theory to the data where n_f is allowed to vary gives a relatively poor χ^2 (6.1) and a very unrealistic value of n_f (0.03). Hence our results indicate that a simple Lorentzian with $\Gamma/E_0=0.32$ provides a significantly better fit to the data than the theoretical results for an Anderson impurity. The most obvious candidate for the cause of this discrepancy is coherence in the $4f$ lattice.

For YbIn$_{0.3}$Ag$_{0.7}$Cu$_4$ our basic result is that the magnetic scattering is inelastic at low temperature, with $E_0=\Gamma$ $=7.5$ meV (87 K). At higher temperatures the power spectrum is quasielastic, and the linewidth increases to a value $\Gamma=10.0$ meV (116 K) at 150 K to a value $\Gamma=13.2$ meV (153 K) at 300 K. The characteristic energy at low temperature is comparable to that deduced from the dc susceptibility

(Fig. 1) but the factor of 1.75 increase in the linewidth between 10 and 300 K is substantially smaller than that suggested by Fig. 1. The data are in accord with theory[11] in that the scattering only becomes quasielastic for $T>T_K$ (87 K). However, the experimentally observed increase in linewidth appears to conflict with theory which suggests that the linewidth should *decrease* by 50% on raising the temperature from 0 to T_K and remain fairly constant for $T_K<T<4T_K$. We note that in YbAgCu$_4$, the linewidth also increases with temperature, but by a smaller factor—from 70 K at low temperature to 90 K at room temperature.[18] The observed increase in linewidth for YbIn$_{0.3}$Ag$_{0.7}$Cu$_4$ is also opposite to what is observed near the valence transition ($x<0.5$) in the alloy system YbIn$_{1-x}$Ag$_x$Cu$_4$, where the Kondo temperature becomes much smaller at high temperature. As mentioned in the Introduction, alloys with $x>0.5$ appear to occur in a region of the phase diagram where the $4f/4f$ interactions that are responsible for the first order valence transition are negligible. Our results suggest that the single-ion Anderson model is inadequate to describe the temperature dependence of the susceptibility and the neutron linewidth even when these interactions are absent. One reason for this may be that the alloys are disordered, with a spectrum of Kondo temperatures on different sites, as recently proposed[19] for UPdCu$_4$.

[1] I. Felner, I. Nowik, D. Vaknin, U. Potzel, J. Moser, G. M. Kalvius, G. Wortmann, G. Schmiester, G. Hilscher, E. Gratz, C. Schmitzer, N. Pillmayr, K. G. Prasad, H. de Waard, and H. Pinto, Phys. Rev. B **35**, 6956 (1987).

[2] J. L. Sarrao, C. D. Immer, C. L. Benton, Z. Fisk, J. M. Lawrence, D. Mandrus, and J. D. Thompson, Phys. Rev. B **54**, 12 207 (1996).

[3] A. L. Cornelius, J. M. Lawrence, J. L. Sarrao, Z. Fisk, M. F. Hundley, G. H. Kwei, J. D. Thompson, C. H. Booth, and F. Bridges, Phys. Rev. B **56**, 7993 (1997).

[4] A. Severing, E. Gratz, B. D. Rainford, and K. Yoshimura, Physica B **163**, 409 (1990).

[5] J. M. Lawrence, S. M. Shapiro, J. L. Sarrao, and Z. Fisk, Phys. Rev. B **55**, 14 467 (1997).

[6] C.-K. Loong, B. H. Grier, S. M. Shapiro, J. M. Lawrence, R. D. Parks, and S. K. Sinha, Phys. Rev. B **35**, 3092 (1987).

[7] E. A. Goremychkin and R. Osborn, Phys. Rev. B **47**, 14 280 (1993).

[8] A. P. Murani, Z. A. Bowden, A. D. Taylor, R. Osborn, and W. G. Marshall, Phys. Rev. B **48**, 13 981 (1993).

[9] S. M. Shapiro, J. D. Axe, R. J. Birgeneau, J. M. Lawrence, and R. D. Parks, Phys. Rev. B **16**, 2225 (1977).

[10] E. Holland-Moritz, D. Wohlleben, and M. Loewenhaupt, Phys. Rev. B **25**, 7482 (1982).

[11] D. L. Cox, N. E. Bickers, and J. W. Wilkins, J. Appl. Phys. **57**, 3166 (1985).

[12] Y. Kuramoto and E. Müller-Hartmann, J. Magn. Magn. Mater. **52**, 122 (1985).

[13] S. M. Shapiro, C. Stassis, and G. Aeppli, Phys. Rev. Lett. **62**, 94 (1989).

[14] A. P. Murani, A. Severing, and W. G. Marshall, Phys. Rev. B **53**, 2641 (1996).

[15] A. P. Murani, J. Phys. C **33**, 6359 (1983).

[16] A. P. Murani and J. Pierre, Physica B **206&207**, 329 (1995).

[17] V. T. Rajan, Phys. Rev. Lett. **51**, 308 (1983).

[18] A. Severing, A. P. Murani, J. D. Thompson, Z. Fisk, and C. K. Loong, Phys. Rev. B **41**, 1739 (1990).

[19] E. Miranda, V. Dobrosavljevic, and G. Kotliar, J. Phys.: Condens. Matter **8**, 9871 (1996).